RESEARCH PAPER

Adsorption of Hydrogen Sulfide (H_2S) by $BaFe_2O_4$-activated Clay Nanocomposite: Preparation and Evaluation

Shadi Sheibani[1], Samira Mandizadeh[2], Seyed Golam Abbas Mousavi[3], Gholamreza Mostafaii[4,*]

[1]Department of Environmental Health Engineering, Faculty of Health, Kashan University of Medical Sciences, Kashan, Iran

[2] Institute of Nano Science and Nano Technology ,University of Kashan, Kashan,Iran

[3] Department of Statistics, Faculty of Health, Kashan University of Medical Sciences, Kashan, Iran

[4] Social Determinants of Health Research Center and Department of Environmental Health Engineering, Faculty of Health, Kashan University of Medical Sciences, Kashan, Iran

ARTICLE INFO

Article History:
Received 24 May 2020
Accepted 06 August 2020
Published 01 December 2020

Keywords:
Adsorption
$BaFe_2O_4$–activated clay
Hydrogen sulfide
Nanocomposite

ABSTRACT

In this study, $BaFe_2O_4$–activated clay nanocomposites were successfully synthesized via mechanosynthesis technique. Structural analysis of the products confirmed the nanoscale formation of nanocomposites. This study focused on adsorption of hydrogen sulfide (H_2S) which is a poisonous gas and can be released from sewage sludge. In the past years, a growing attention in the usage of adsorptive desulfurization in industrial applications has been observed due to its many benefits such as low cost. Nanocomposites were characterized by scanning electron microscopy (SEM), energy dispersive X-ray (EDS) analysis, Fourier transform infrared (FTIR), X-ray powder diffraction (XRD). Results showed different loading of barium ferrite in nanocomposite is important for adsorption rate. Furthermore, adsorption rate of hydrogen sulfide was improved by increasing $BaFe_2O_4$- activated clay concentration which was confirmed by statistical results. The highest average of removal efficiency was 92.79±0.90 in the concentration of 300 $g.L^{-1}$and loading 6%. We could recycle $BaFe_2O_4$–activated clay nanocomposite, 3 times without a significant decrease in activity.

How to cite this article
Sheibani S., .Mandizadeh S., Mousavi S.G.A., Mostafaii Gh. Adsorption of Hydrogen Sulfide (H2S) by $BaFe_2O_4$-activated Clay Nanocomposite: Preparation and Evaluation. J Nanostruct, 2020; 10(4): 838-845. DOI: 10.22052/JNS.2020.04.017

INTRODUCTION

Recently, $BaFe_2O_4$ nanostructure has received increased attention due to the unique physical and chemical properties. $BaFe_2O_4$ nanostructure can be utilized in many fields such as sensors and catalysts [1,2]. To date, $BaFe_2O_4$ have been broadly used to modify of support surfaces such as silicon rubber [3]. Among the supporting materials, activated clay is the best candidate because of its appropriate acidity and super adsorption capability.

In recent years, the widespread demand of hydrogen sulfide is responsible for environmental pollutions, H_2S is a colorless gas with a rotten egg smell. This gas is extremely toxic, corrosive and flammable. Great amount of H_2S is found in biological and industrial gases that causes corrosion in the pipes and other equipment [4]. Releasing of hydrogen sulfide is a physical/chemical process which is occurred in wastewater treatment system. H_2S can seriously threat the human health [5]. Hence, control of gas emission is necessary not only for the public health and safety but also for protecting the environment [6]. To

* *Corresponding Author Email: mostafai_gr@kaums.ac.ir*

Table 1 Preparation conditions, morphology, particle sizes of as-prepared samples.

Sample	Metal oxide-Zeolite nanocomposite	Percentage of ferrite	Morphology	*Average particle size (nm)
Sample 1	$BaFe_2O_4$	-	Agglomerate	100-155
Sample 2	$BaFe_2O_4$	-	Agglomerate	74-100
Sample 3	Toncile-$BaFe_2O_4$	2	Semi-spherical	92-79
Sample 4	Toncile-$BaFe_2O_4$	4	Agglomerate	86-153
Sample 5	Toncile-$BaFe_2O_4$	6	Agglomerate	68-161

date, different methods and techniques have been developed to control the odor such as chemical scrubbers, burning the odorant compounds, adsorption, biological methods including biofilters, trickling biofilters, bio scrubbers and activated sludge reactors [7-10].

Among the different methods for H_2S removal, absorption is very effective because of its simplicity, efficiency, flexibility and sensitive to toxic pollutants [11]. Recently, mesoporous materials such as active carbon and silica can be used as adsorbent due to the amazing adsorption ability. Furthermore, the results of several studies showed that using small particles, specially in the nanometer scale, makes a significant improvement in the process of removing pollutants. Dagaonkar indicated that adding nanometer particles of titanium oxide (TiO_2) to different supports increased absorption of CO_2 gas [12]. In other study Mostafaii et al, showed that zinc oxide nanoparticles can remove coliforms in the concentration of 1.1 gr/L at 90 min [13]. Labrada et al. removed some amount of hydrogen sulfide using nano TiO_2 and ZnO [14]. Khaleghi et al., indicated benzenesulfonic acid-graphene (BS-rGO) nano absorbent could remove hydrogen sulfide [15]. Sub Song et al. showed that nanoparticles of zinc oxide/reduced graphite oxide composite could remove a significant amount of hydrogen sulfide gas [16]. Nour et al. showed silver / polydimethylsiloxane (PDMS) nanocomposite has excellent activity for H_2S gas removal [17]. Mandizadeh et al. reported desulfurization efficiency can be improved by using barium ferrite nanoparticles ($BaFe_{18}O_{18}$) [18].

In the present work, $BaFe_2O_4$, combined with activated clay nanocomposites were prepared by procedure method for removing hydrogen sulfide. This research aims to achieve high desulfurization from wastewater by ferrite-activated clay nanocomposite. Nanocomposites were characterized by scanning electron microscopy (SEM), Fourier transform infrared (FTIR), energy dispersive X-ray (EDS) analysis, and X-ray powder diffraction (XRD).

MATERIALS AND METHODS

The starting cationic sources, Ba $(NO_3)_2$ (M_w: 261.337 $g.mol^{-1}$), $Fe(NO_3)_3.9H_2O$ (Mw: 404 $g.mol^{-1}$, Glucose (Mw: 180.156 $g.mol^{-1}$) and activated clay were purchased from Sigma-Aldrich. All chemicals were supplied in analytical grades and utilized without further purification.

Preparation of barium ferrite with auto-combustion sol-gel

For synthesis barium ferrite with auto-combustion sol-gel, specific amount of Ba $(NO_3)_2$ (0.2 gr), $Fe(NO_3)_3.9H_2O$ (3gr) and glucose (4.2gr) were dissolved in the minimum amount of distilled water. The mixture was heated to the temperature of 100°C. After the evaporation all water, gel was dried and calcined at 700°C. The preparation conditions are summarized in Table 1.

Preparation of activated clay

We placed 10 g of clay in a three-necked flask with a solution of HNO_3 and H_2SO_4 in 1 to 3 stoichiometric ratio. Flask was at a controlled temperature of 85˚C for 3 h. Then, the extra acid was decanted and washed 5 times with distilled water. Finally, it was dried at 100°C for 3 hours.

Preparation of $BaFe_2O_4$-activated clay nanocomposite

Nanocomposites of monoferrite- activated clay were prepared by mechanosynthesis technique. This experiment occurred on the FRITSCH planetary mill brand. A ratio of activated silica and nanoferrite (2,4 and 6%) were added to the flask and mixed at 400 rpm for 3 h. Finally, the product was washed with deionized water and dried at room temperature. All of the preparation conditions were illustrated in Table 1. Regeneration of nanocomposites was performed at 200^0C in air.

Catalytic evaluation

We prepared a model sample from Kashan University of Medical sciences wastewater with

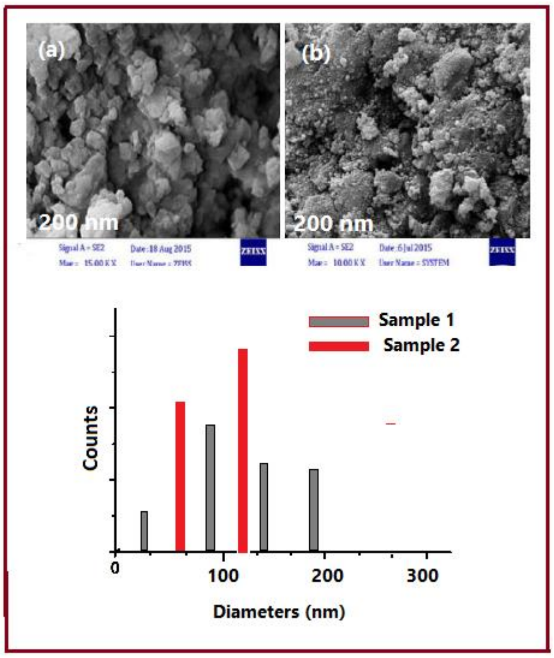

Fig. 1. FESEM micrographs of nanoferrite (a) sample 1, (c) sample 2

a specific amount of sulfur compound. In order to measure the sulfur amount in the wastewater, Petrotest Calorimetric Bomb C5000 according to ASTM D-1266 was used. The flask was joined to a reflux- system with nanocomposite in the absorbent column at the temperature 60-100°C. In this study, different concentration of nanocomposites were investigated. The removal efficiency of hydrogen sulfide was calculated by the following formula:

$$\frac{A-B}{A}\times 100 \quad (1)$$

A: Sulfur amount in the real sample
B: Sulfur amount of the product

Characterization

EDX analysis was performed using Philips Scanning Electron Microscope model EM208 equipped with x-ray spectroscopy. Microscopic morphology of the samples was characterized by Philips Electron Microscope model XL-30ESEM. FT-IR spectra were recorded on Magna-IR, spectrometer 550 Nicolet in KBr pellets in the range of 400–4000 cm^{-1}. The XRD pattern was recorded from diffractometer of the Philips Company with X'PertPro monochromatized Cu Kα radiation (λ = 1.54 Å)

RESULTS AND DISCUSSION

Morphology

Morphology of samples were characterized by SEM images. Fig. 1a is related to the prepared $BaFe_2O_4$ without glucose (Sample 1). We observed in Fig 1a that the as-prepared monoferrites have spherical morphology. The conjunction of particles is due to the magnetic properties of ferrite. Fig 1b is related to the synthesized $BaFe_2O_4$ in the presence of glucose (Sample 2). Using sugar, semi-spherical particles formed, in a homogeneous texture because of the presence of hydroxyl and carboxylic acid group as capping agents. From its respective particle histograms, the average sizes of nanostructures are in the range of 36-72 nm. The Fig.2 shows the SEM of barium ferrite-activated clay nanocomposites. Fig. 2a,b and c are related to Sample 3, Sample 4 and Sample 5, respectively. As results, we observed regular arrangement of nanostructures for all samples. .The results from morphological observations are tabulated in Table 1.

Structural analysis

Phase type, crystal structure, product purity and the size of crystalline grains were measured by XRD pattern. Fig.3a,b and c are related to Sample 3, Sample 4 and Sample 5 respectively. In Fig 2a the diffraction peaks in 2θ=22.89^0, 26.60^0, 29.21^0,

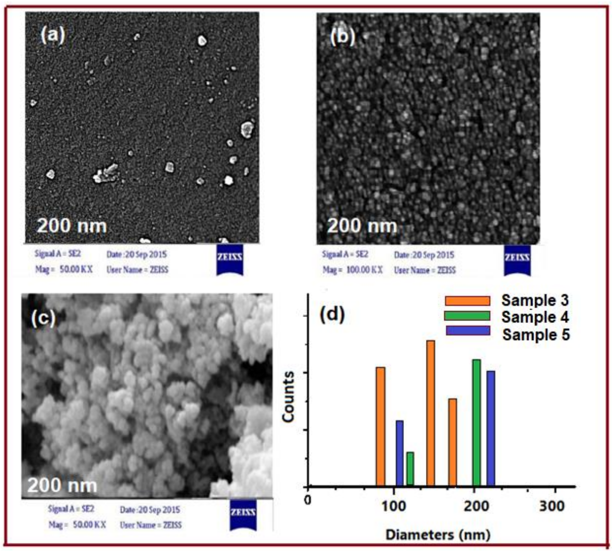

Fig. 2. FESEM micrographs of nanocomposites (a) sample 3, (b) sample 4 (c) sample 5

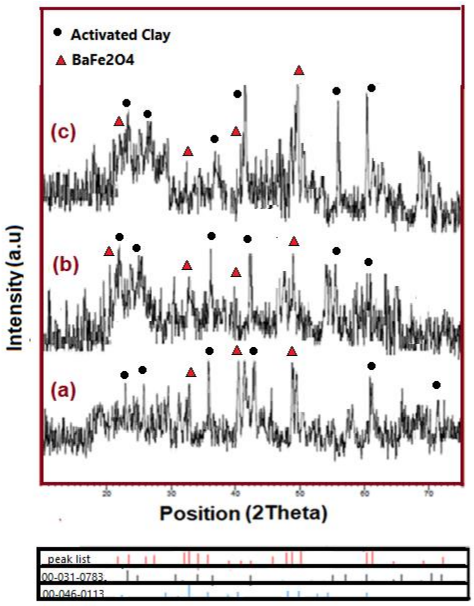

Fig. 3. XRD patterns of as-prepared nanocomposites; (a) sample 3, (b) Sample 4, (c) sample 5

and 43.95^0 are related to activated clay with the standard diffraction pattern (JCPDS Card Nos. 00-031-0783). Other diffraction peaks of Sample 3 related to $BaFe_2O_4$ (JCPDS Card Nos. 00-046-0113) growth at 23.3°, 33.2^0, 40.1^0 and 49.36^0. As shown in Fig 3, for all samples, no peaks were detected as impurities and high purity of the products were observed. Sharp peaks in the diffraction pattern are due to the high crystallization of the achieved products. Using the Scherrer equation [18], the crystal size of $BaFe_2O_4$ were 30, 35, 48 nm for Sample 3, Sample 4 and Sample 5 respectively.

EDX and FT-IR

Fig.4a shows EDX spectrum of barium ferrite-activated clay nanocomposites (Sample 5). This spectrum shows the presence of Ba, Fe, O, Si and Al in the product. According to the results, the high purity of the product was observed. Fig 4b shows FT-IR spectra of barium ferrite- activated clay nanocomposites (Sample 5). The important peaks were observed at 3421.75, 1653.67 and 1031.80

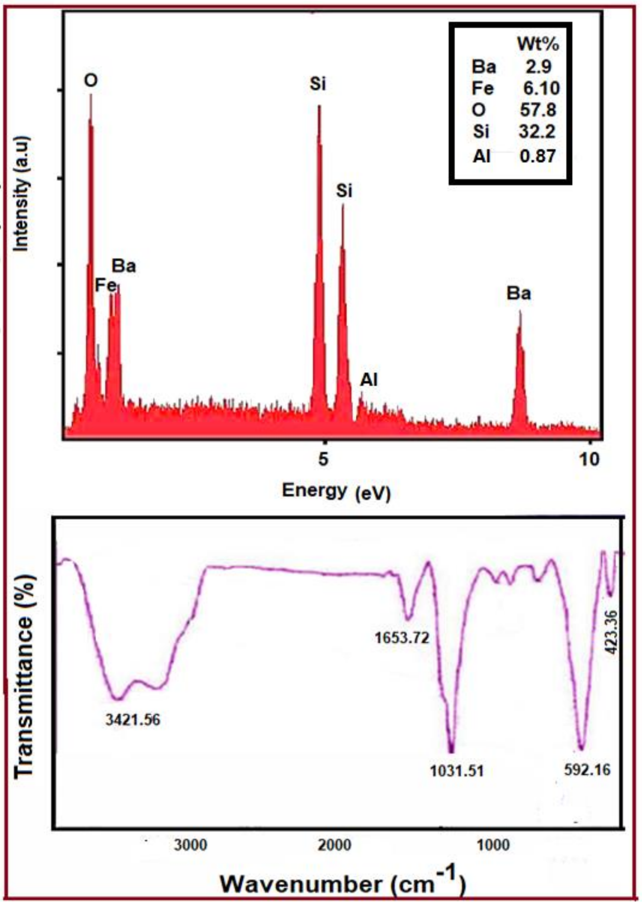

Fig.4. (a) FT-IR spectrum (b) EDX from sample 5

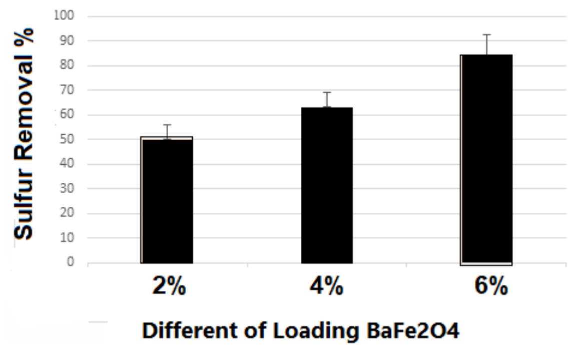

Fig. 5. Average efficiency percentage of Hydrogen sulfide removal in different concentrations

cm^{-1}, are related to mode stretching O-H, Si=O and C-O respectively. Two intense bands of 592.57 and 423.95 cm^{-1} are related to the stretching vibration Fe-O and Ba-O, respectively.

Desulfurization efficiency

Effect of varying concentration and loading of barium ferrite for desulfurization efficiency and its statistics study

According to Fig.5, by increasing loading of barium ferrite in nanocomposite, removal efficiency of hydrogen sulfide was increased. The average efficiency for hydrogen sulfide removal in 3 different loading of barium ferrite with F=413.07

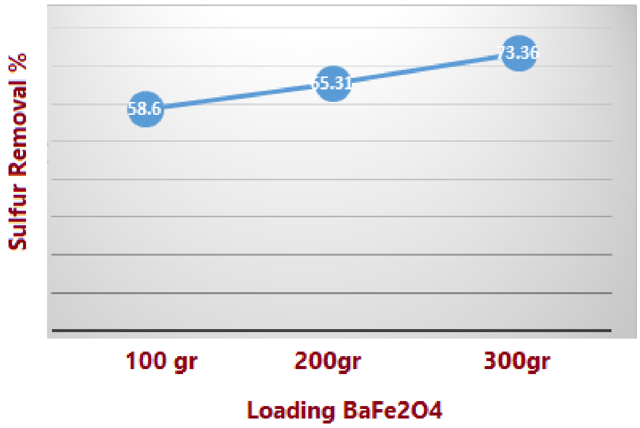

Fig.6. Average efficiency percentage of Hydrogen sulfide removal in different weights

Table 2: Average removal efficiency percentage of Hydrogen sulfide in different weights and concentrations

Different Loading (%)			Concentration ($gr.L^{-1}$)
6%	4%	2%	
	$\bar{x}$±SD		
74.46 ±4.51	58.40 ±0.93	42.94 ±1.13	100
84.98 ±2.02	60.80 ±0.90	50.14 ±0.52	200
92.79 ±0.90	70.41 ±5.37	56.90 ±0.68	300

and sig<0.001 showed a statistically significant difference. The results indicated a significant difference (P<0.001) between the nanocomposites in loading 2 and 4%, 2 and 6% and 4 and 6%. Hence, the $BaFe_2O_4$- activated clay nanocomposite can be utilized as a new adsorbent for sulfur removal. On the other hand, the existence of metal ion (barium) in nanocomposite can be enhanced the adsorption properties. It seems that porosity of activated clay and the reaction between iron with sulfur are two main reasons for desulfurization efficiency. Deep desulfurization removal from wastewater is reported by Pourreza et al. They showed by increasing of dopting molybdenum oxide from 10 to 50%, sulfur removal was increased due to chemical and physical adsorption [19-21]. In other study, Liua et al., indicated by increasing loading activated carbon in compacted kaolin (6%), absorption capacity was enhanced [22]. Compared to other studies, $BaFe_2O_4$- activated clay nanocomposite (6%) has strong potential for adsorptive desulfurization.

As shown in Fig. 6 increasing of $BaFe_2O_4$-activated clay nanocomposite concentration from 100 $ge.L^{-1}$ to 300 $gr.L^{-1}$ improved the adsorption rate of hydrogen sulfur from wastewater. The adsorption rate of sulfur compound in 300 $gr.L^{-1}$ nanocomposite was estimated about 73.36% for 30 min. The average removal efficiency in 3 different concentration with F=76.45 and sig<0.001 showed a statistical significant difference. The results of the comparison of two concentrations showed a significant difference between the different loading of 2 and 4%, 2 and 6% and 4 and 6% (P<0.001). The results of one-way ANOVA with independent variables of concentration and the dependent variable of removal efficiency showed (F=215.96, sig<0.001), (F=11.89, sig=0.008) (F=30.08, sig<0.001) for different loading 2%, 4% and 6% respectively.

The highest removal efficiency can be obtained in the loading of 6% and the concentration of 300 $gr.L^{-1}$ (92.79%) (Table 2). Two-way ANOVA with different concentration, loading and sulfur removal efficiency had no statistical significance with F=2.264 and sig=0.102. In one study, Guanghua Xia et al., showed hydrogen sulfide can be removed from viscose fiber wastewater by using biological trickling filter (BTF) that was in associated with our results. In industrial processes, production

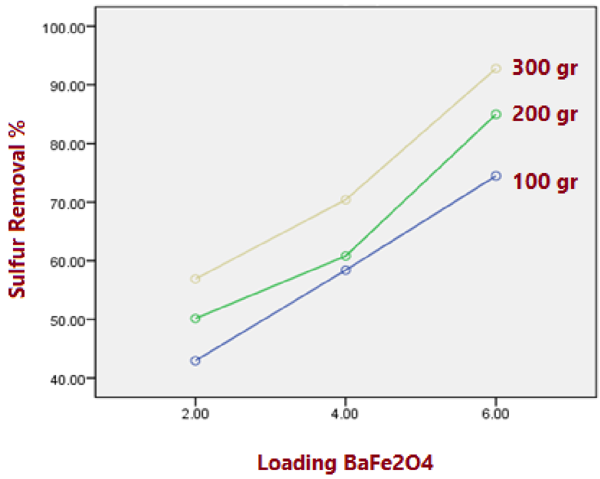

Fig. 7. Average removal efficiency percentage of Hydrogen sulfide in different weights and concentrations

shut down, power failure or repair of electrical equipment are important problems. These can reduce the enzyme activities for desulfurization process [23] while in our study, these problems can not stop nanocomposite activity.

Also, according to Fig.7, the average removal hydrogen sulfide for the concentration of 100, 200 and 300 $gr.L^{-1}$ and the different loading of 2, 4 and 6% were investigated. Loading of 2% had the lowest removal efficiency while the loading of 6% had the highest efficiency.

To date several studies have been reported for hydrogen sulfide removal by nanocomposites such as GO-ZnO and zinc oxide-MWCNT nanocomposites [24-25]. Among the different studies, our study has some advantages such as having a simple method for synthesis nanocomposites (auto-combustion sol gel), and simple method for desulfurization.

CONCLUSION

In summary, barium monoferrite nanostructures have been synthesized successfully by auto-combustion sol-gel method. It is understood that by choosing the glucose as capping agent and 700°C and 2 h for calcination temperature and time, barium monoferrite can be obtained. Then $BaFe_2O_4$- activated clay nanocomposites were prepared by mechanosynthesis technique

Adsorptive desulfurization results showed barium monoferrite- activated clay nanocomposite is one of the best candidates for sulfur removal. Increasing loading barium ferrite from 2 to 6% can promote adsorption rate of hydrogen sulfide from wastewater in concentration 300 $gr.L^{-1}$ which was confirmed by statistical results.

ACKNOWLEDGMENTS

This study has been prepared based on the research plan number 97145 approved by the Research Affairs of Kashan University of Medical Sciences whose funds has been used. Here by, the authors would like to extend their deepest gratitude to the chancellor of the Research Department, and honorable Head of the faculty of Health and honorable vice chancellor of the faculty of Health.

CONFLICT OF INTEREST

The authors declare that there is no conflict of interests regarding the publication of this manuscript.

REFERENCES

1. Galvão WS, Neto DMA, Freire RM, Fechine PBA. Super-Paramagnetic Nanoparticles with Spinel Structure: A Review of Synthesis and Biomedical Applications. Solid State Phenomena. 2015;241:139-76.
2. Mandizadeh S, Salavati-Niasari M, Sadri M. Hydrothermal synthesis, characterization and magnetic properties of BaFe2O4 nanostructure as a photocatalytic oxidative desulfurization of dibenzothiophene. Separation and Purification Technology. 2017;175:399-405.
3. Peymanfar R, Rahmanisaghieh M. Preparation of neat and capped BaFe2O4 nanoparticles and investigation of morphology, magnetic, and polarization effects on its microwave and optical performance. Materials Research Express. 2018;5(10):105012.
4. Geng Q, Wang L-J, Yang C, Zhang H-Y, Zhao Y-R, Fan H-L, et al. Room-temperature hydrogen sulfide removal with zinc oxide nanoparticle/molecular sieve prepared by melt infiltration. Fuel Processing Technology. 2019;185:26-37.

5. Kim H, Lee H, Choi E, Choi I, Shin T, Im H, et al. Characterization of odor emission from alternating aerobic and anoxic activated sludge systems using real-time total reduced sulfur analyzer. Chemosphere. 2014;117:394-401.
6. Van der Heyden C, Demeyer P, Volcke EIP. Mitigating emissions from pig and poultry housing facilities through air scrubbers and biofilters: State-of-the-art and perspectives. Biosystems Engineering. 2015;134:74-93.
7. Gabriel D, Deshusses MA, Gamisans X. Desulfurization of Biogas in Biotrickling Filters. Air Pollution Prevention and Control: John Wiley & Sons, Ltd; 2013. p. 513-23.
8. Qiu X, Deshusses MA. Performance of a monolith biotrickling filter treating high concentrations of H2S from mimic biogas and elemental sulfur plugging control using pigging. Chemosphere. 2017;186:790-7.
9. Arellano-García L, González-Sánchez A, Van Langenhove H, Kumar A, Revah S. Removal of odorant dimethyl disulfide under alkaline and neutral conditions in biotrickling filters. Water Science and Technology. 2012;66(8):1641-6.
10. Talaiekhozani A, Bagheri M, Goli A, Talaei Khoozani MR. An overview of principles of odor production, emission, and control methods in wastewater collection and treatment systems. Journal of Environmental Management. 2016;170:186-206.
11. Nagpal M, Kakkar R. Use of metal oxides for the adsorptive removal of toxic organic pollutants. Separation and Purification Technology. 2019;211:522-39.
12. Ma M, Zou C. Effect of nanoparticles on the mass transfer process of removal of hydrogen sulfide in biogas by MDEA. International Journal of Heat and Mass Transfer. 2018;127:385-92.
13. Mostafaii G, Chimehi E, Gilasi H, Iranshahi L. Investigation of Zinc Oxide Nanoparticles Effects on Removal of Total Coliform Bacteria in Activated Sludge Process Effluent of Municipal Wastewater. Journal of Environmental Science and Technology. 2016;10(1):49-55.
14. Valdes Labrada GM, Kumar S, Azar R, Predicala B, Nemati M. Simultaneous capture of NH3 and H2S using TiO2 and ZnO nanoparticles - laboratory evaluation and application in a livestock facility. Journal of Environmental Chemical Engineering. 2020;8(1):103615.
15. Khaleghi Abbasabadi M, Rashidi A, Khodabakhshi S. Benzenesulfonic acid-grafted graphene as a new and green nanoadsorbent in hydrogen sulfide removal. Journal of Natural Gas Science and Engineering. 2016;28:87-94.
16. Song HS, Park MG, Kwon SJ, Yi KB, Croiset E, Chen Z, et al. Hydrogen sulfide adsorption on nano-sized zinc oxide/reduced graphite oxide composite at ambient condition. Applied Surface Science. 2013;276:646-52.
17. Nour M, Berean K, Chrimes A, Zoolfakar AS, Latham K, McSweeney C, et al. Silver nanoparticle/PDMS nanocomposite catalytic membranes for H 2 S gas removal. Journal of Membrane Science. 2014;470:346-55.
18. Mandizadeh S, Sadri M, Salavati-Niasari M. Sol–gel auto combustion synthesis of BaFe18O27 nanostructures for adsorptive desulfurization of liquid fuels. International Journal of Hydrogen Energy. 2017;42(17):12320-6.
19. Pourreza A, Askari S, Rashidi A, Fakhraie S, Kooti M, Shafiei-Alavijeh M. A highly efficient MIL-101(Cr)–Graphene–molybdenum oxide nano composite for selective oxidation of hydrogen sulfide into elemental sulfur. Journal of Industrial and Engineering Chemistry. 2019;71:308-17.
20. Bromberg L, Diao Y, Wu H, Speakman SA, Hatton TA. Chromium(III) Terephthalate Metal Organic Framework (MIL-101): HF-Free Synthesis, Structure, Polyoxometalate Composites, and Catalytic Properties. Chemistry of Materials. 2012;24(9):1664-75.
21. Chen C, Zhang M, Guan Q, Li W. Kinetic and thermodynamic studies on the adsorption of xylenol orange onto MIL-101(Cr). Chemical Engineering Journal. 2012;183:60-7.
22. Liu HW, Feng S, Leung AK. Effects of nano-activated carbon on water and gas permeability and hydrogen sulphide removal in compacted kaolin. Applied Clay Science. 2019;172:80-4.
23. Xia G, Zhou X, Hu J, Sun Z, Yao J, Chen D, et al. Simultaneous removal of carbon disulfide and hydrogen sulfide from viscose fibre waste gas with a biotrickling filter in pilot scale. Journal of Cleaner Production. 2019;230:21-8.
24. Ghayedi A, Khosravi A. Laboratory investigation of the effect of GO-ZnO nanocomposite on drilling fluid properties and its potential on H2S removal in oil reservoirs. Journal of Petroleum Science and Engineering. 2020;184:106684.
25. Singh A, Pandey V, Bagai R, Kumar M, Christopher J, Kapur GS. ZnO-decorated MWCNTs as solvent free nano-scrubber for efficient H2S removal. Materials Letters. 2019;234:172-4.